JOURNAL OF MATERIALS SCIENCE 10 (1975) 1697–1710

Continuous precipitation in Cu-rich Cu-Ti binary and Cu-Ti-Al ternary alloys

T. K. VAIDYANATHAN, K. MUKHERJEE
Polytechnic Institute of New York, 333 Jay Street, Brooklyn, New York, USA

An investigation has been carried out to study precipitation in a Cu–4% Ti binary and a Cu–2.1% Ti-2.4% Al ternary alloys which develop modulated microstructures upon ageing. Precipitate-free zones near the grain boundaries were observed on ageing immediately below a critical temperature representing the transition from the coherent to the incoherent region of the coherent phase diagram. In addition, a pronounced tendency for elastic interaction between the precipitate particles was detected, giving rise to aligned groups of precipitates containing a maximum of eight or nine particles in each group. At least near this critical temperature, decomposition occurs in the metastable region of the coherent phase diagram rather than in the spinodal region. The formation of the modulated structures in these alloys is, therefore, considered to arise not necessarily through spinodal decomposition. Continuous precipitation in a Cu–2.1% Ti–5% Al alloy is shown to result in spherical particles with no alignment. The effect of Al addition on the coherent solvus temperature is discussed in terms of a vacancy solute interaction mechanism.

1. Introduction

Cu-rich binary Cu–Ti and ternary Cu–Ti–Al alloys are known to show remarkable potential for precipitation hardening [1–4]. In both cases precipitation results in modulated structures. The mechanism responsible for the development of modulated structures in the binary Cu–Ti alloys has been recently attributed to spinodal decomposition [5, 6]. Further experimental evidence is desirable to help clarify the nature of the decomposition in the binary and ternary alloys. This is because these alloys also satisfy the necessary conditions for the development of modulated structures through the classical nucleation and elastic interaction mechanism, similar to those reported for Ni–Al and Ni–Ti [7] alloys and this possibility needs further elucidation. While the tensile properties of Cu–Ti binary alloys have received some attention in the past [2, 8], more extensive data over a wider range of temperatures are thought necessary. Although some important features of precipitation in Cu–Ti–Al ternary alloys have been studied by resistivity and optical microscopy [9, 10], the mechanical properties and the microstructural features of the developing stages of the precipitation in these alloys have not been reported previously.

2. Experimental

The alloys were prepared from 99.999% pure Cu and Al and 99.97% pure iodide crystal grade Ti supplied by the United Mineral and Foote Mineral Corporation respectively. Melting was carried out in an MRC arc melter using non-consumable tungsten electrode after evacuating the furnace chamber and backfilling with argon to provide an argon atmosphere during melting. A titanium getter was used during the melting. To ensure sufficient homogenization in the alloy, melting was repeated at least three times. The button so obtained was again melted and cast into a rectangular flat ingot (for further cold-rolling into 4 mil* thick sheets for electron microscopic studies) or into a cylindrical ingot (for further cold swaging to rods having a diameter of 0.100 in. (2.5 mm) for tensile studies). All ingots were homogenized at 890° C for 40 h in a vacuum furnace under a vacuum of 10^{-7} Torr. Spectro-

* 1 mil = 2.54×10^{-5} m.

graphic analysis on typical samples gave the following compositions:

Alloy	% Ti	% Al	% Cu
1	3.99	–	balance
2	2.03	2.35	balance
3	2.14	4.90	balance.

The oxygen content in all alloys was less than 50 ppm.

All ageing was carried out with the specimens encapsulated in evacuated quartz tubing (10^{-6} Torr). The sheet samples were solution-treated at 890° C for 40 min and aged isothermally. These samples were electropolished using the window technique with an electrolyte of 2 parts methanol and 1 part nitric acid by volume, at a temperature of less than −40° C. The cathodes were nichrome wires would into the form of a helix. The cold swaged rods were machined into tensile specimens having a gauge diameter of 0.050 in. (1.25 mm) and a gauge length of 0.50 in. (12.5 mm). The specimens were solution-treated and aged as before and tensile tested with an Instron Universal testing machine at a nominal strain-rate of about 1.2×10^{-4} sec^{-1}. All tests were performed at room temperature.

3. Experimental results

3.1. Yield strength isotherms

Fig. 1 gives plots of yield strength (0.2% offset) against isothermal ageing time of the Cu–4% Ti alloy. Some noteworthy features of these curves are:

(1) at the lower temperature of 400° C, the yield strength increases continuously with ageing time for nearly 7500 min. There is, however, a fast initial increase of yield strength with ageing time followed by a more gradual increase at the later states. Although this is not readily apparent from the curves because of the logarithmic time scale, it can be seen that the first 1000 min ageing at 400° C appears to result in an increase of 46 000 psi* over the solid solution yield strength of 51 000 psi, whereas the subsequent ageing to peak yield strength for an additional 6500 min corresponds to a further increase of only 7000 psi;

(2) the maximum yield strength developed at 400° C is in excess of 100 000 psi. The peak yield strengths at 500 and 600° C are 96 000 and 89 000 psi, respectively;

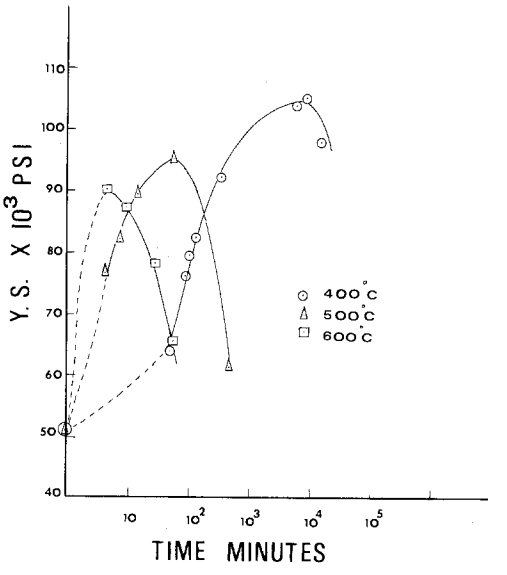

Figure 1 Yield strength versus time for the Cu–4% Ti binary alloy. Isothermal ageing curves.

(3) the elongation of 25% at the as-quenched state is reduced to about 10%, 12% and 14% respectively on ageing to peak yield strength at 400, 500 and 600° C, respectively.

The ageing response of the Cu–2.1% Ti–2.4% Al alloy shows a similar trend as seen in Fig. 2. However, a lower peak yield strength on ageing at similar temperatures. The maximum yield strength developed on ageing at 400, 500 and 600° C are 76 000, 66 000 and 57 000 psi, respectively. The elongation was, however, con-

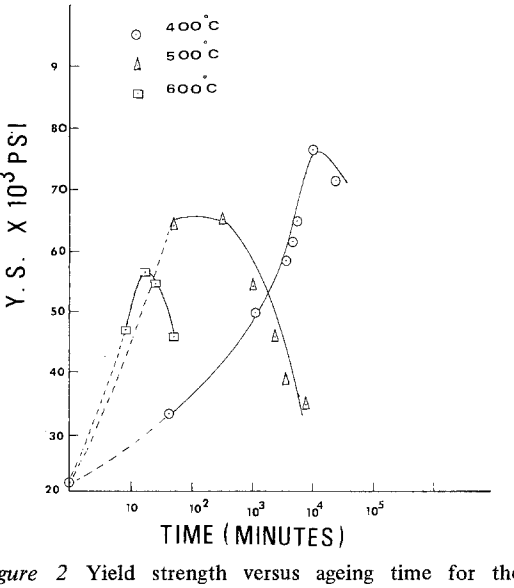

Figure 2 Yield strength versus ageing time for the Cu–2.1% Ti–2.4% Al alloy. Isothermal ageing curves.

* 10^3 psi ≡ 6.89 N mm^{-2}.

sistently higher, i.e. 30% at the as-quenched state as compared to 13% at the highest yield strength condition.

In the case of the Cu–2.1% Ti–5% Al alloy, the ageing behaviour shows some remarkable differences (Fig. 3). Thus, the peak yield strength of 72 000 psi is realized in this alloy on ageing at 400° C for a comparatively shorter period of 2800 min. Also, no significant change in yield strength could be detected on ageing at the higher temperatures of 500 and 600° C. The elongation data varied from 20% at the maximum yield strength condition to 35% at the as-quenched state.

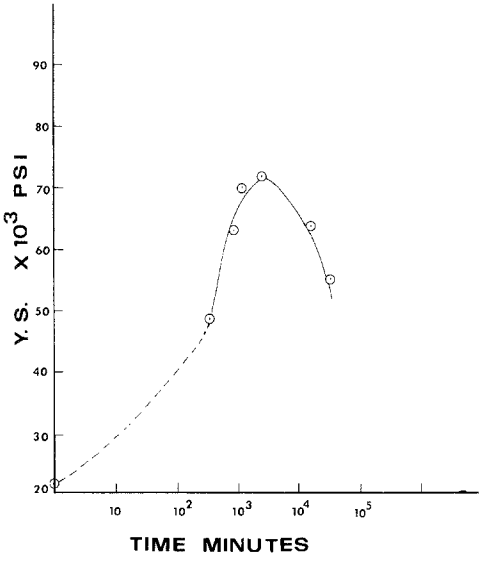

Figure 3 Yield strength versus time for the Cu–2.1% Ti–5% Al alloy aged at 400° C.

3.2. Electron microscopy

3.2.1. Cu–4% Ti alloy

The solution-treated and quenched alloy specimen showed only a very faint contrast, possibly of a second phase, but did show distinct contrast of stacking faults and dislocations such as in Fig. 4. The streaking of the matrix reflections in the SAD of Fig. 4b is in the ⟨1 1 1⟩ directions typical of faults. No extra reflections were observed irrespective of foil orientation. On the other hand, the alloy sample aged for 8 h at 450° C, such as those of Fig. 5 showed well-developed modulated structures and superlattice reflections (arrowed in the figure). These superlattice reflections are identical to those reported by Knights and Wilkes [11] and Laughlin and Cahn [12] in Cu–Ti alloys with lesser Ti content.

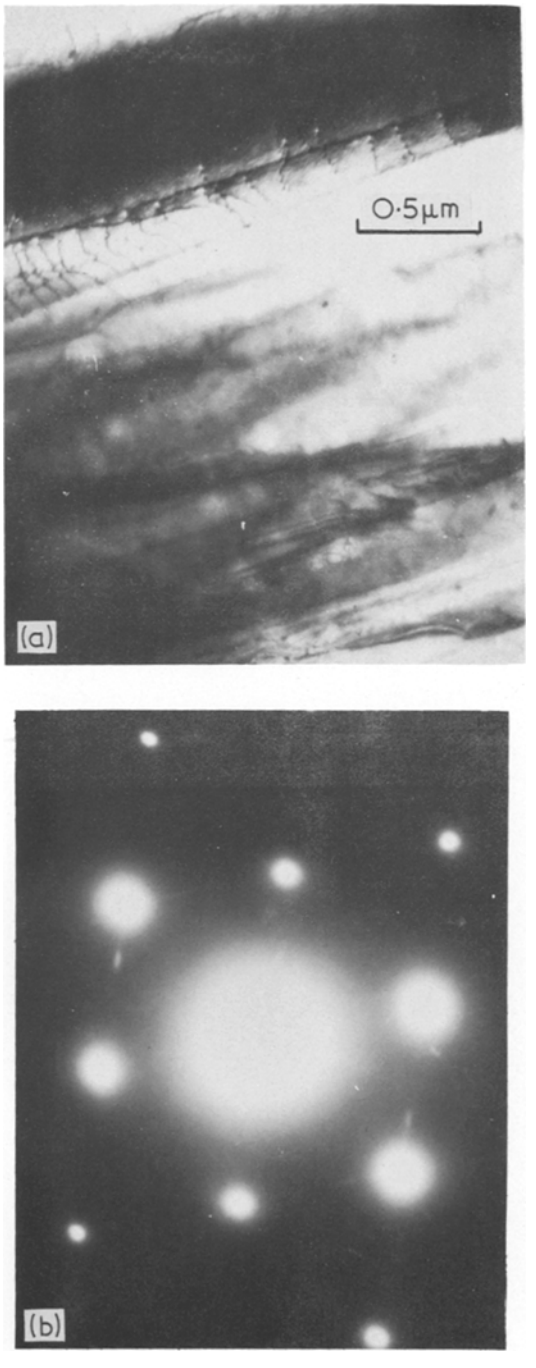

Figure 4 Cu–4% Ti alloy, solution-treated and quenched. (a) BF. (b) Associated SAD. [1 1 0] Z.A.

Fig. 6 shows a series of electron micrographs of alloys aged at different degrees of undercooling as represented by different ageing temperatures. It can be seen that there is a marked tendency for precipitate alignment. The precipitate distribution is also nearly uniform in the micrographs (a to e)

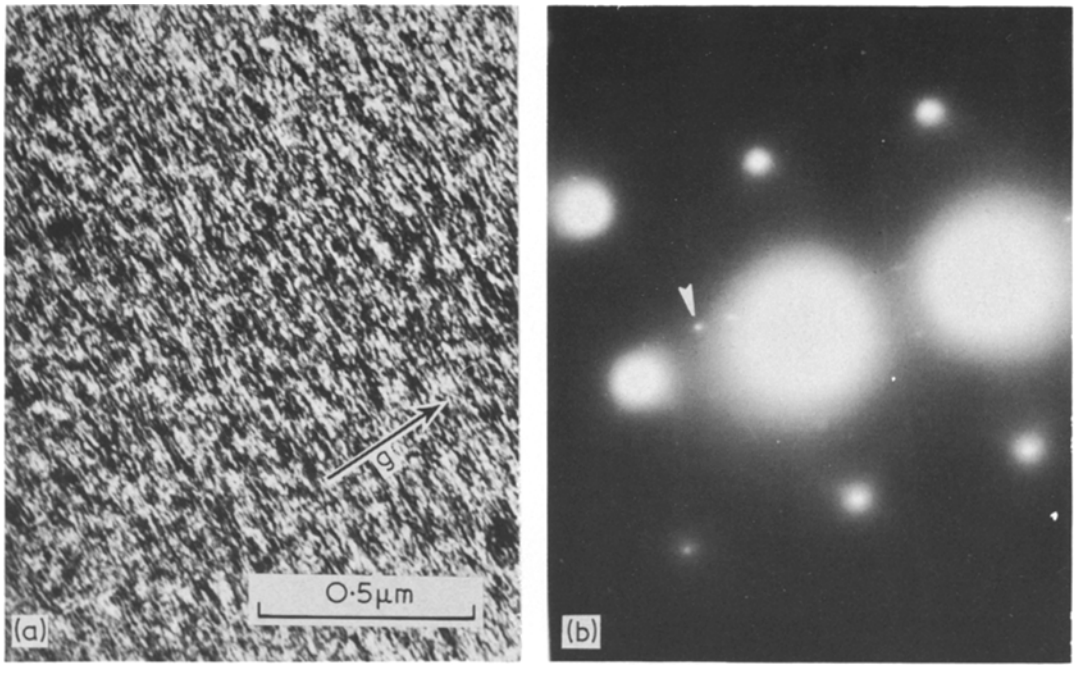

Figure 5 Cu–4% Ti alloy, aged 8 h at 450° C. (a) BF. (b) Associated SAD. Foil nearly normal to [0 1 0]. $\bar{g} = [0\,0\,\bar{2}]$.

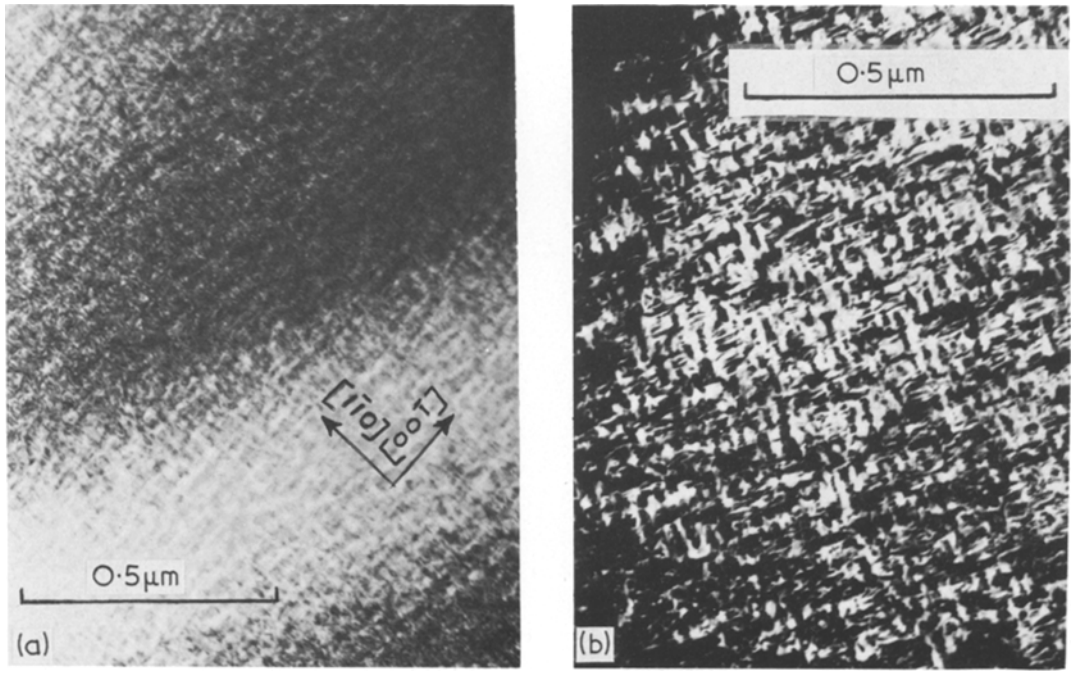

Figure 6 Cu–4% Ti alloy, precipitate distribution on ageing at different degrees of undercooling. (a) 400° C, 24 h, BF. (b) 500° C, 2 h, BF. (c) 600° C, 15 min, BF. (d) 650° C, $4\frac{1}{2}$ min, BF. (e) Same as (d), DF from matrix reflection. (f) 700° C, 30 min, BF. Observe the δ-fringes imaged by the fundamental reflections of the matrix due to the coherent precipitate-matrix interfaces e.g. (c), (d) and (e). Also observe the loss of coherency in (f) and the appearance of interfacial dislocations. Foil nearly normal to [1 1 0] in all cases.

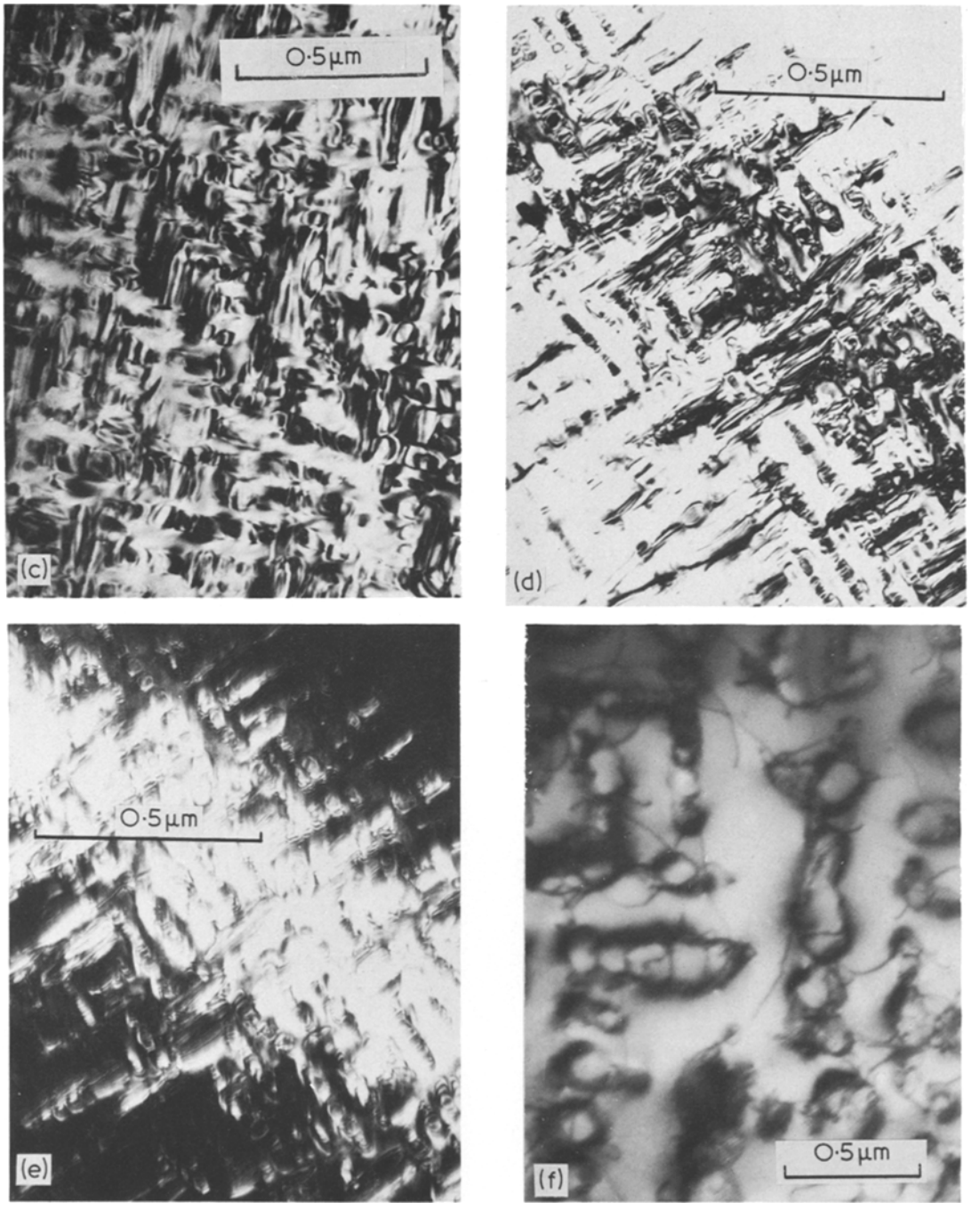

Figure 6 continued.

of Fig. 6. However, in Fig. 6f, the precipitate distribution is not uniform and, in addition, groups of precipitate aligned in the ⟨1 0 0⟩ directions form, similar to those reported by Ardell and Nicholson [7] in Ni–Al alloys. This indicates that elastic interaction between the particles is intimately involved in the precipitate alignment process. Figs. 6f and 7 show loss of coherency of the continuous precipitate in this alloy. Because of the discontinuous precipitation which occurs collateral to the continuous precipitation, the detection of such loss of coherency is extremely difficult in this alloy, as reported by earlier investigators [2, 6].

Figure 7 Cu–4% Ti alloy, aged at 700° C for 30 min Moiré fringes in contrast.

3.2.2. Cu–2.1% Ti–2.4% Al alloy

The solution-treated, as-quenched Cu–2.1% Ti–2.4% Al alloy showed no second phase contrast on thin foil examination. The ageing kinetics of precipitate formation and growth on ageing at 500° C can be seen in Fig. 8a to e. The earliest stages of the microstructure in this alloy show remarkable similarity to that of the binary Cu–4% Ti alloy, as seen from Figs. 6a and 8a. However, on prolonged ageing, a strong tendency for the formation of groups of precipitates aligned in the ⟨1 0 0⟩ directions is manifest in this alloy more markedly than in the case of the binary alloy. On ageing for 160 h, the maximum number of particles in each group is roughly 8 or 9 and is reminiscent of the ogdoadically diced cubes (i.e. a group of eight cubes arranged in a master cube) observed in Ni-base alloys by Westbrook [13]. Ardell and Nicholson [7] have pointed out that such ogdoad formation is a natural consequence of the elastic interaction between precipitate particles. Fig. 9 shows a non-uniform precipitate distribution and the early stages of the influence of such elastic interaction on precipitate alignment, indicating that classical nucleation and

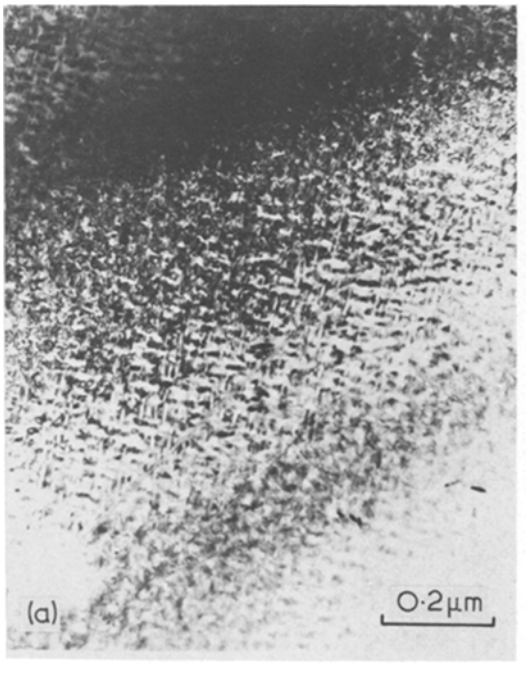

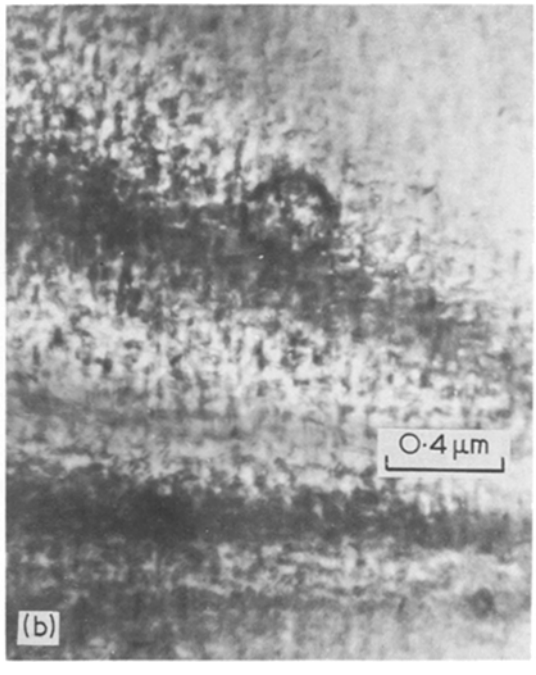

Figure 8 Cu–2.1% Ti–2.4% Al alloy, stages of precipitate development on ageing at 500° C. (a) 1 h, BF. (b) 6 h, BF. (c) 48 h, BF. (d) 72 h, BF. (e) 160 h, BF. (f) Same area as (e), DF from matrix reflection. Foil nearly normal to [1 0 0] in all cases.

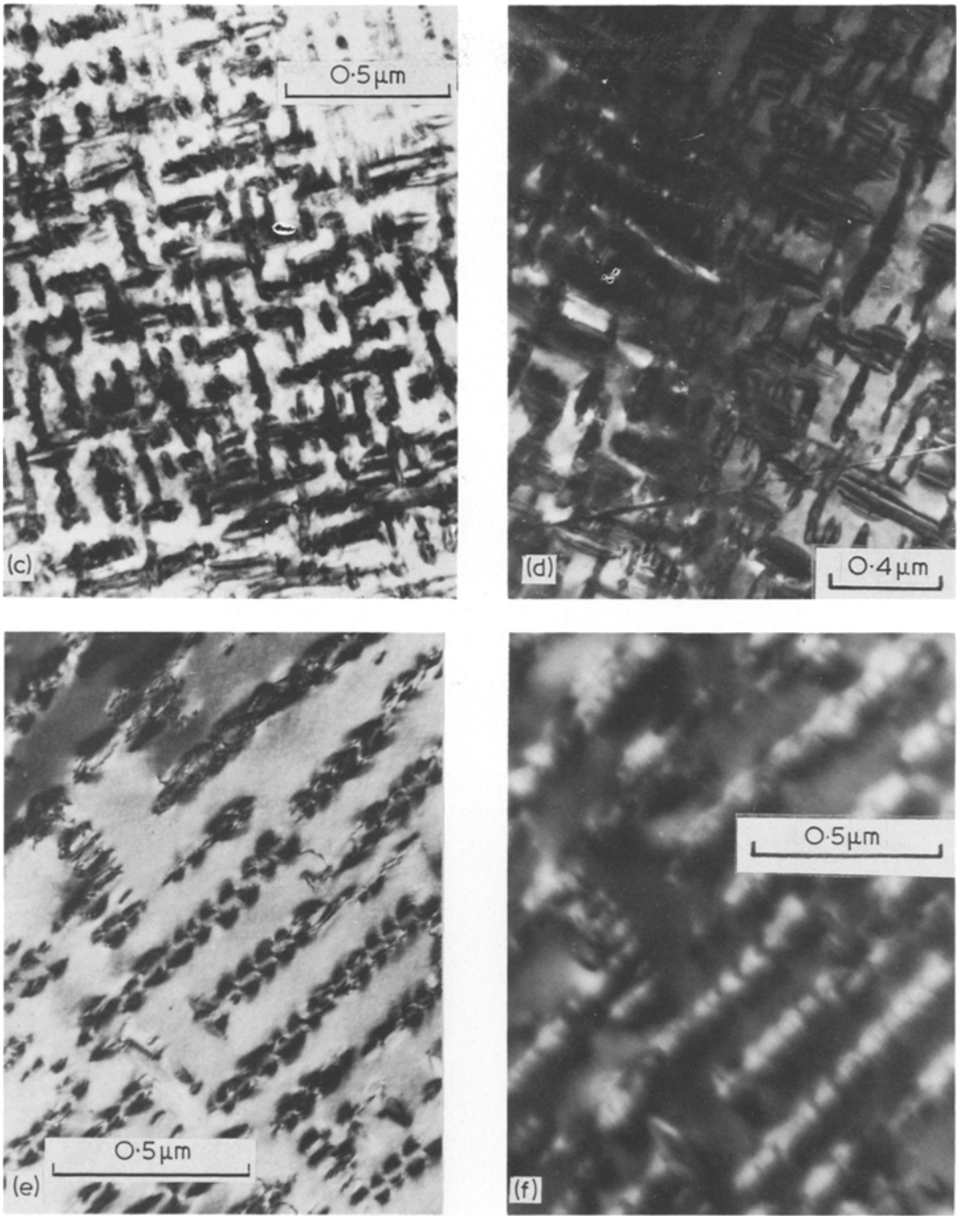

Figure 8 continued.

elastic interaction are the more likely origin of the modulated structures in this alloy at the higher ageing temperatures of $\geqslant 500^{\circ}$ C.

3.2.3. Cu–2.1% Ti–5% Al alloy

A solution-treated, quenched alloy showed extended dislocations indicative of a low stacking-fault energy, as in Fig. 10. On ageing the alloy at 400° C, continuous precipitation is seen as in Fig. 11. The nearly parallel lines of no contrast indicate a spherical strain field. This, together with the X-ray evidence reported in a similar alloy composition by Korotayev *et al.* [9], indicate that low coherency strains develop during the early

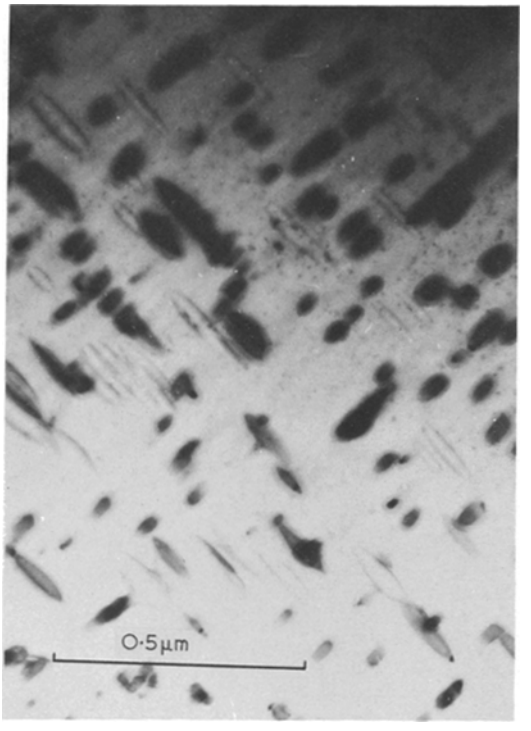

Figure 9 Cu–2.1% Ti–2.4% Al alloy, aged 1 h at 600° C. BF. Observe the non-uniform precipitate distribution. Also note that the alignment is in the initial stages.

stages of precipitation in this alloy. The absence of periodicity and alignment in the precipitate distribution is reminiscent of similar behaviour in Cu–Co alloys and can be attributed to the low coherency strains discussed above. On further ageing up to 120 h, precipitate coarsening is seen in Fig. 12a. The associated SAD in Fig. 12b shows split {1 1 1} spots and indicates loss of cubic symmetry in agreement with the tetragonal crystal structure reported for the equilibrium precipitates in the ternary Cu–Ti–Al alloys [10].

3.2.4. Grain-boundary regions

Since the precipitate distribution at or near grain-boundary regions can provide useful information on the mechanism of precipitation, these regions were of particular interest in this study.

On ageing the Cu–4% Ti alloy at temperatures $\leqslant 650°$ C, segments of grain boundaries with no precipitates at the grain boundaries were observed. In addition, no precipitate-feee zones (PFZ) could be detected. However, on ageing at 700° C, incoherent equilibrium precipitates at the grain boundaries (different in morphology and growth pattern from discontinuous precipitates) were observed as in Fig. 13a. In addition, Fig. 13b shows a PFZ near a grain boundary towards the

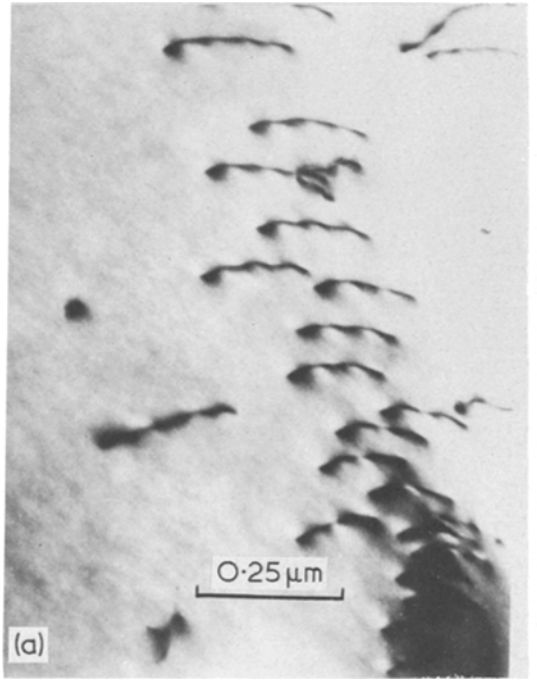

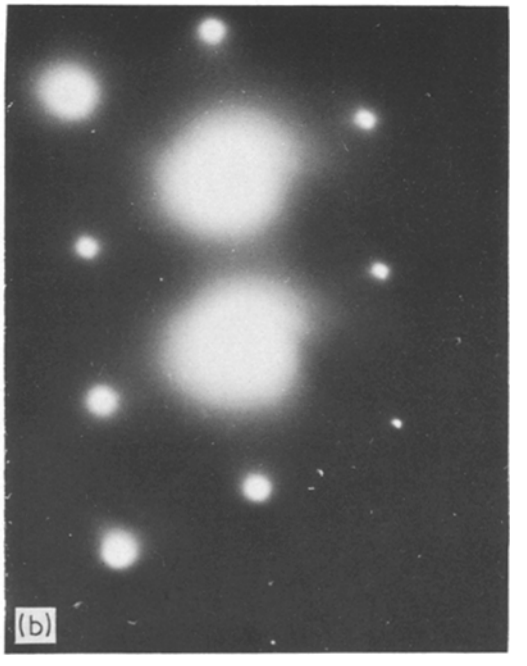

Figure 10 Cu–2.1% Ti–5% Al alloy, solution-treated and quenched. (a) BF. (b) Associated SAD. [1 1 0] Z.A. $\bar{\mathbf{g}} =$ [1 1 1].

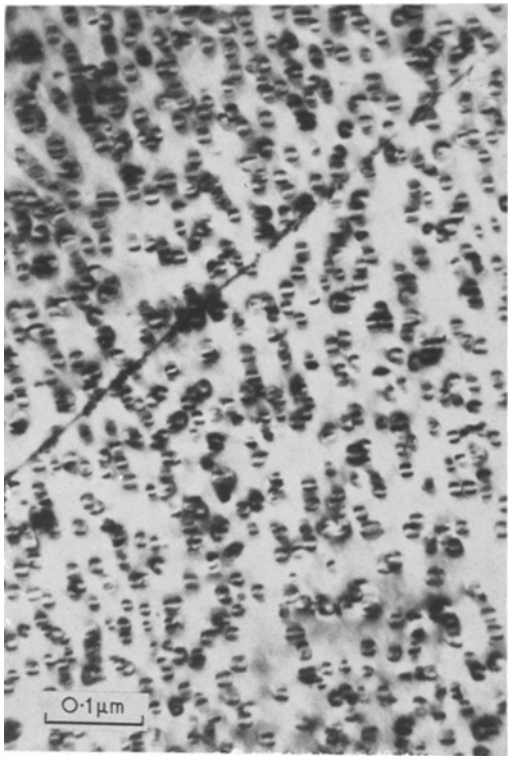

Figure 11 Cu–2.1% Ti–5% Al alloy, aged 25 h at 400° C. BF.

region showing continuous precipitate. Thus, despite the obscuring effect of discontinuous precipitate formation and propagation from the grain boundaries in the alloy, it was possible to detect the formation of PFZs near grain-boundary regions.

In the Cu–2.1% Ti–2.4% Al alloy, however, no discontinuous precipitation was observed. This made it possible to examine several grain-boundary regions at different ageing conditions. Fig. 14a is such a region and shows continuous precipitates in the grain interior with equilibrium precipitates at the grain boundaries. Observe the absence of any PFZ adjacent to the grain boundary. On ageing at 600°C, however, coarse grain-boundary precipitates and wide PFZs are seen as in Fig. 14b. The total width of the PFZ on both sides of the grain boundary exceeds 1 μm. It is well known that such wide PFZs are also observed in some Al-base alloys, such as Al–Zn–Mg [14] in which GP zones form. Precipitation inside such PFZs have also been reported in the past and are further confirmed in this alloy through double ageing treatments (Fig. 15). Observe that the precipitates are coarser in size and distribution nearer the PFZ in Fig. 15 indicating the similarity of these PFZs to those of the Al-base alloys in which the origin of

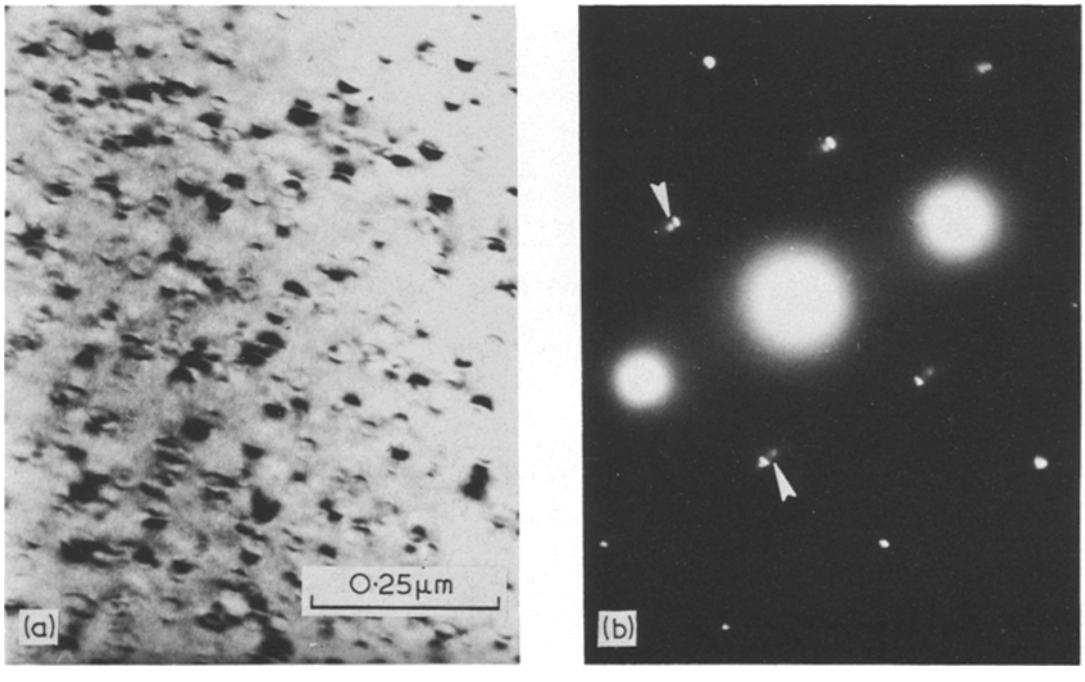

Figure 12 Cu–2.1% Ti–5% Al alloy, aged 120 h at 400° C. (a) BF (b) Associated SAD. [1 1 0] Z.A. Note the split (1 1 1) spots due to the loss of cubic symmetry.

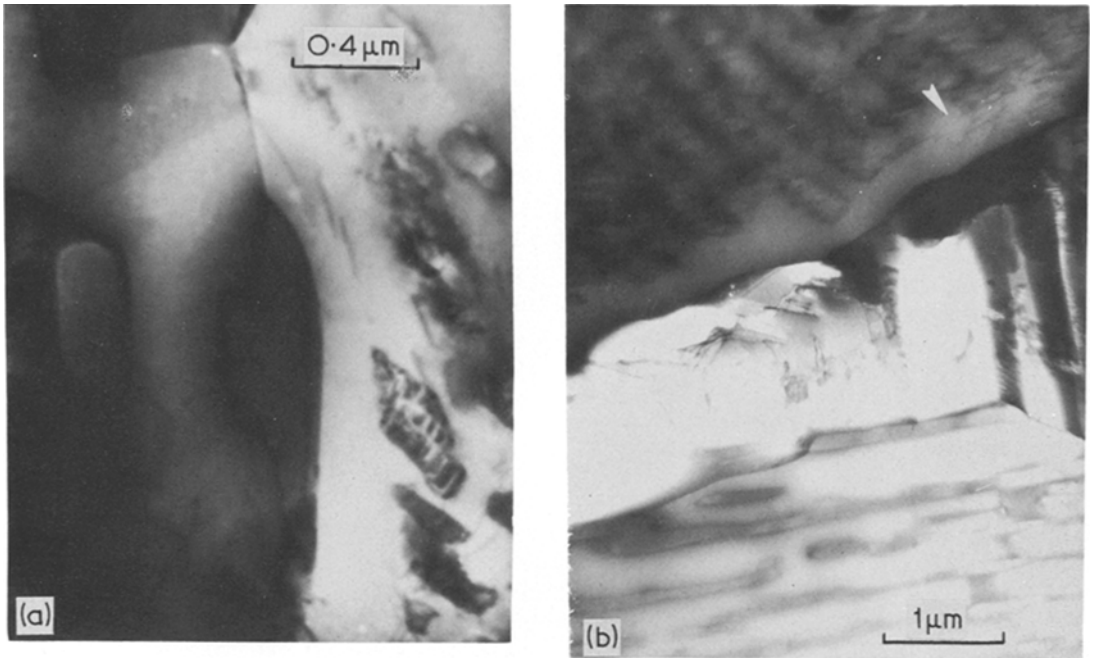

Figure 13 Cu–4% Ti alloy, aged at 700° C, 30 min. (a) BF. Shows incoherent equilibrium precipitates at the grain boundaries. (b) BF. Shows a PFZ near the grain boundary towards the continuous precipitates in one of the grains. Also shows discontinuous precipitates in other grain.

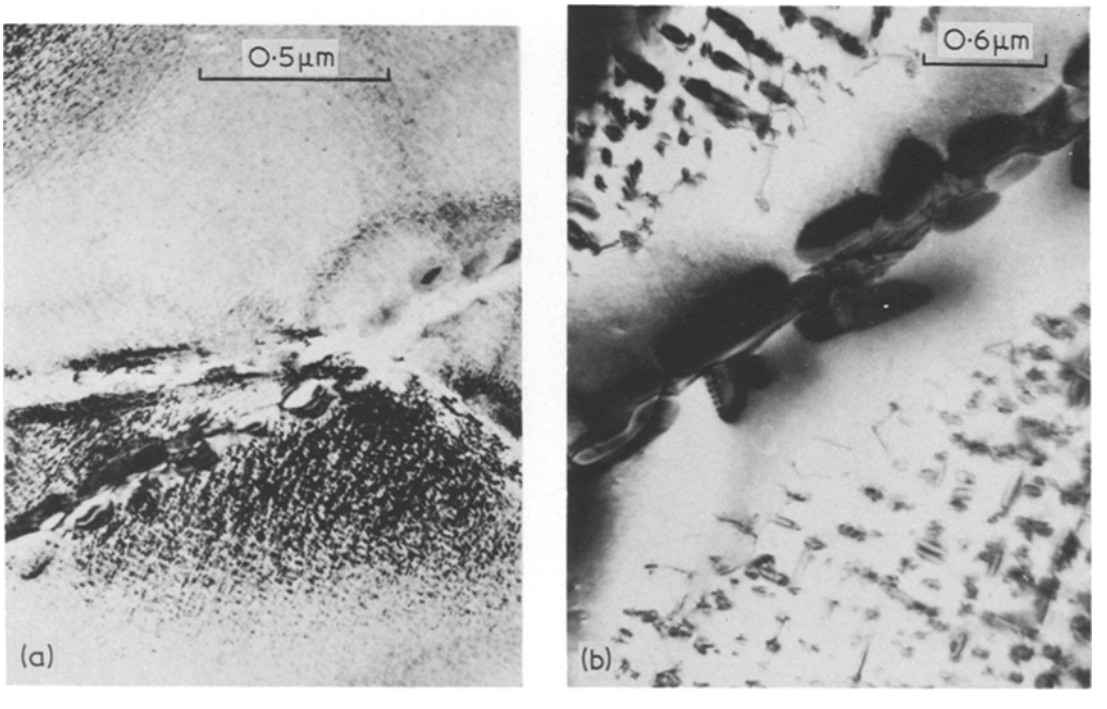

Figure 14 Cu–2.1% Ti–2.4% Al alloy, shows influence of undercooling below the coherent solvus temperature on the occurrence of PFZ. (a) BF, aged 24 h at 400° C. (b) BF, aged 1 h at 600° C. PFZ width ~ 10 000 Å.

Figure 15 Cu–2.1% Ti–2.4% Al alloy, aged 100 min at 600° C and 45 h at 400° C. BF. Observe the wide PFZ of the initial ageing at 600° C and the subsequent precipitation inside this PFZ region during the lower temperature ageing.

these PFZs have been attributed to the role of point defects in addition to solute depletion effects. The temperatures at which the double ageing treatments are carried out are critically important as can be seen in Fig. 16 where the initial ageing at 620° C appears to have resulted in no continuous precipitates and, therefore, no initial PFZ. The second ageing treatment at 400° C does, however, result in a PFZ as a result of the vacancy flux (and the associated solute flux) to the grain-boundary sinks that actually occurred in the first ageing treatment. These observations point to the conclusion that the first ageing treatment in this alloy was above the coherent solvus temperature of the alloy. An interesting micrograph is Fig. 16b and shows the grain interior in a region where the initial ageing at 600° C resulted in a somewhat moderately spaced distribution of equilibrium precipitates and as a result, the solute depletion effects around these precipitates resulted in a tendency for precipitation to occur on dislocations. On the other hand, the solute depletion effect is observed as a precipitate-free zone around a single equilibrium precipitate in Fig. 16c. Since sufficient solute supersaturation is important to ensure homogeneous nucleation, the above tendencies for precipitation on dislocations and occurrence of denuded zones are easily understood. Fig. 17 is the result of ageing the alloy clearly above the coherent solvus temperature at 650° C and shows complete absence of continuous precipitates. Incidentally, the incoherent precipitates of Fig. 17 shows an internal structure at A probably because of faults in the Al-rich precipitates of low stacking-fault energy.

In the Cu–2.1% Ti–5% Al alloy, wide PFZs were observed even at 400° C. At the higher ageing temperatures of 500° and 600° C, only localized precipitation at the grain interior and grain boundaries was observed and continuous precipitation was completely absent. However, a tendency for the vacancies to form dislocation loops (with faults at the centre due to the low stacking-fault energy of the alloy) and helical dislocations through climb of screw dislocations was observed, as seen in Fig. 18.

4. Discussion of results

4.1. Development of modulated structures

An important feature of the Cu-rich region of the Cu–Ti phase diagram is the sharp drop of Ti solubility in Cu with temperature. Thus while the Ti solubility in Cu is more than 7 at.% at 890° C, this drops to 2 at.% at 700° C, 0.6 at.% at 500° C and 0.4 at.% at 400° C [15]. Thus the solute supersaturation increases markedly over a small temperature range of undercooling and, consequently, isothermal ageing at $\leqslant 650°$ C ensures a high degree of solute supersaturation. In addition, the strain parameter $\eta = (1/a)(da/dc)$ is also nearly 10% in this alloy [5]. As a result, there is a strong tendency for precipitate alignment in Cu–4% Ti alloy, on ageing at $\leqslant 650°$ C as discussed in Section 3.1.2. It is not surprising, then, that previous investigators have tended to attribute the initial stages of ageing to spinodal decomposition because both the alignment at the very early stages of ageing and the near uniform precipitate distribution are suggestive of such a possibility. However, two features observed during this investigation, on ageing at 700° C, necessitate

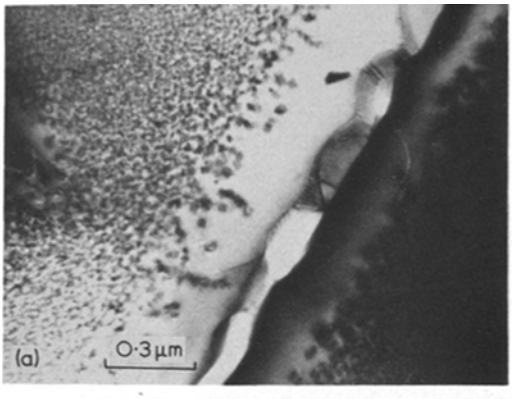

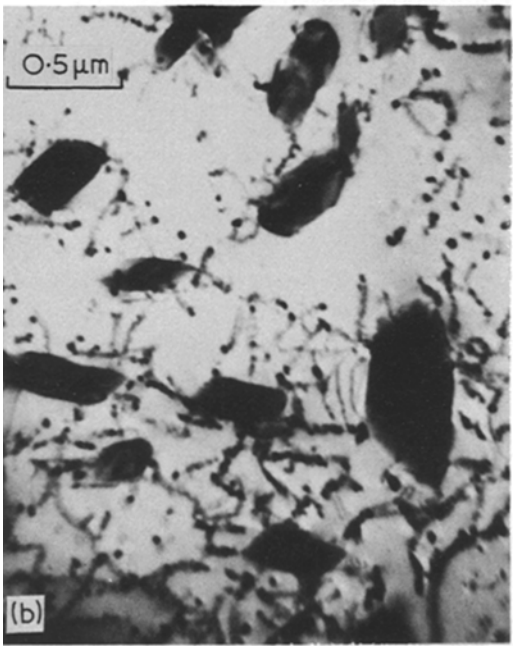

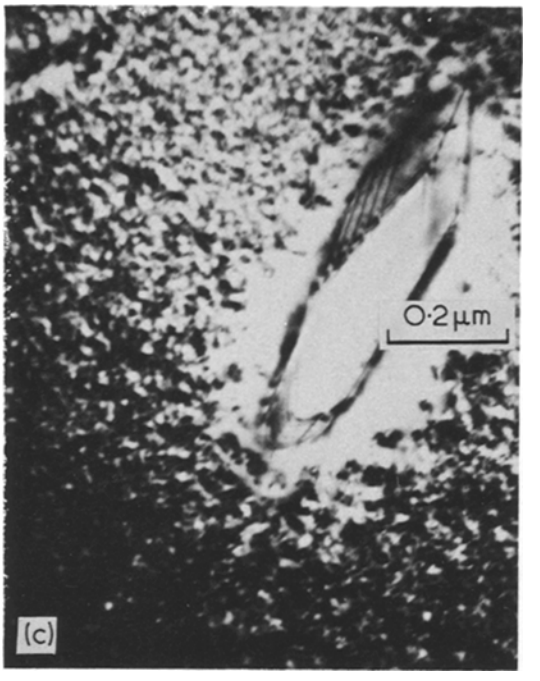

Figure 16 Cu–2.1 Ti–2.4% Al alloy, aged at 620° C for 100 min and 45 h at 400° C. (a) BF. Grain-boundary region. Observe the absence of discontinuous precipitates on ageing at 620° C. (b) BF, grain interior. Observe the precipitation on dislocation during the second ageing at 400° C in the regions adjacent to the coherent equilibrium precipitates formed at 620° C. (c) BF. Precipitate free zone around an equilibrium precipitate.

an argument in favour of an alternative origin for the modulated structures in this alloy. These features are:

(1) there is a strong tendency for particles to form groups aligned in the ⟨1 0 0⟩ directions;

(2) incoherent equilibrium precipitates form at the grain boundaries and PFZs occur adjacent to the grain boundaries. In the case of the Cu–2.1% Ti–2.4% Al alloy, these features are even more markedly observed as seen in Section 3.2.3. In addition, the precipitate distribution in the Cu–2.1% Ti–2.4% Al alloy at the early stages of ageing at 600° C is non-uniform, thus ruling out spinodal decomposition at this temperature.

The first feature of the tendency to form groups of precipitates on ageing in certain temperature ranges in both the Cu–4% Ti binary alloy and the Cu–2.1% Ti–2.4% Al ternary alloy decidedly point to the role of elastic interaction between the particles in the alignment process. This behaviour, therefore, puts the modulated structures of the binary Cu–Ti and ternary Cu–Ti–Al alloys in the same class as that of Ni-base alloys investigated in detail by Ardell and Nicholson [7]. Accordingly, the formation of the modulated structures in the Cu–4% Ti and Cu–2.1% Ti–2.4% Al alloys is not necessarily due to spinodal decomposition.

The second feature, namely the occurrence of incoherent precipitates at the grain boundaries and of PFZs adjacent to the grain boundaries in these alloys containing modulated structure, also tends to further confirm that the modulated structures in these alloys do not necessarily result from spinodal decomposition. Lorimer and Nicholson [16] have suggested a nucleation theory for the formation of GP zones in Al-base alloys. The motivation for this theory arose as a result of the extensive PFZs observed in these alloys near a critical temperature below which the GP zones

Figure 17 Cu–2.1% Ti–2.4% Al alloy, aged 1 h at 650° C BF. Observe the absence of discontinuous precipitation. Observe the internal structure of precipitates, probably due to faulted character.

form. Since the nature of the precipitates change from the coherent type to the incoherent type on altering the ageing temperature across this critical temperature, they have suggested that this temperature is the coherent solvus temperature of the alloy. This suggestion is also in agreement with the marked change of precipitate distribution on ageing the alloy just below and just above this critical temperature. Since the coherent precipitates form through homogeneous nucleation and the incoherent precipitates form through localized precipitation (which arise as a result of heterogenous nucleation at sites of lower activation energy barrier), such a change of precipitate distribution across the coherent solvus is readily understood. The Cu–4% Ti alloy and the Cu–2.1% Ti–2.4% Al alloy studied in this investigation also conspicuously show the above features, namely the occurrence of wide PFZs just below a critical temperature and the sharp change of precipitate nature and distribution across this critical temperature. The modulated structures that develop immediately below this critical temperature is, therefore, best ascribed to decomposition inside the metastable region of the coherent phase diagram rather than in the spinodal region. Since precipitation occurs through nucleation in this region, the modulated structures in these alloys

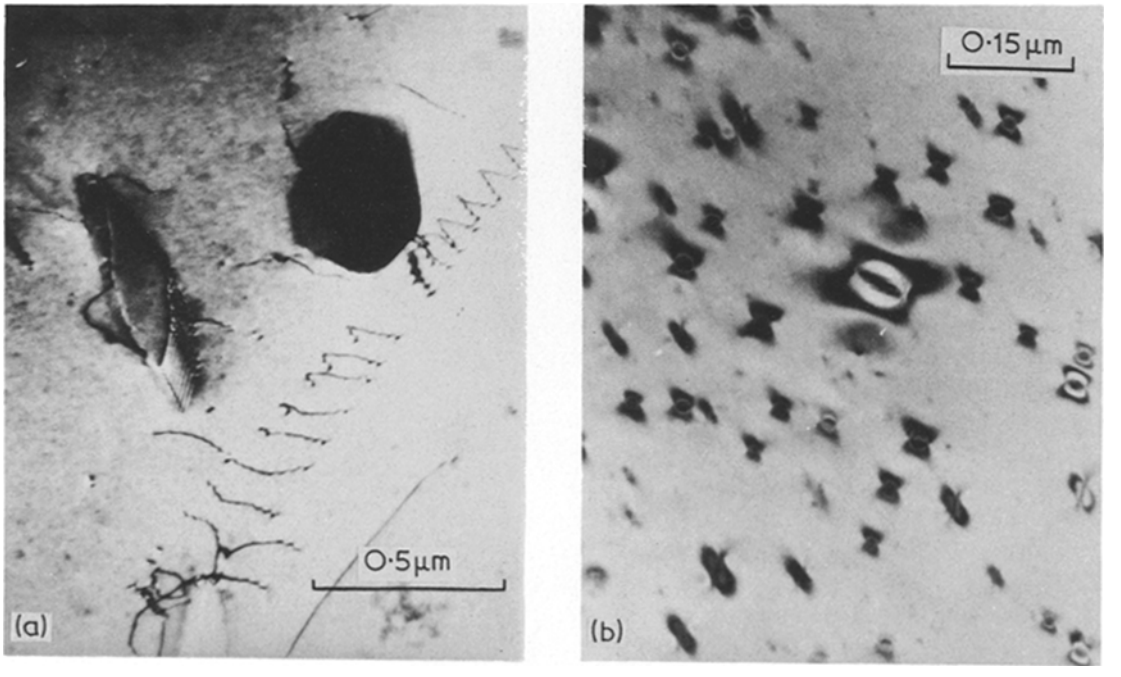

Figure 18 Evidence for vacancy condensation in the Cu–2.1% Ti–5% Al alloy. (a) BF, aged 72 h, at 500° C. Note helical dislocation formed by climb of screw dis-location through vacancy condensation. (b) BF, aged at 600° C for 260 min. Faulted loops formed via vacancy condensation and collapse.

may arise through classical nucleation and elastic interaction and not necessarily through spinodal decomposition. It is felt, therefore, that the recent suggestion of Hilliard [17] to exercise caution in attempting to characterize the development of modulated structures through a unique mechanism such as spinodal decomposition is well worth repetition at this stage.

4.2. Influence of Al on continuous precipitation in Cu–Ti alloys

From the nature of precipitate distribution at various ageing temperatures shown in Section 3, and other observations in the course of this study, it can be concluded that the coherent solvus temperatures of the Cu–4% Ti, Cu–2.1% Ti–2.4% Al, and Cu–2.1% Ti–5% Al alloys are in the vicinity of 720, 620 and 450° C, respectively, although an exact determination of these temperatures was not attempted. This conclusion is also in agreement with the results of the reversion experiments of Korotayev *et al.* [9], through resistivity curves. In this study, three alloys with the composition of Cu–4.7% Ti (alloy 1), Cu–2.3% Ti–2% Al (alloy 2) and Cu–2.3% Ti–5% Al (alloy 3) were initially aged at 350° C for various times and then upquenched to 500° C and aged. The results showed that partial reversion occurred in alloys 1 and 2 and complete reversion took place in alloy 3. Since complete reversion occurs across the metastable coherent solvus, the observation of complete reversion in alloy 3 is in agreement with the conclusion in this investigation that the coherent solvus temperature is in the vicinity of 450° C for this alloy. On the other hand, the partial reversion in alloys 1 and 2 may arise due to the fact that some of the embryos formed at 350° C are of subcritical size at 500° C, although both of the ageing temperatures are below the critical temperature for these alloys. While the supercritical embryos would be stable, the subcritical embryos would redissolve at 500° C, thus accounting for partial reversion. A wide cluster size distribution is to be expected under isothermal ageing conditions.

The change of coherent solvus with Al content discussed above is also associated with a change of the vacancy solute interaction in these alloys. Thus the complete absence of dislocation loops and helical dislocations in the Cu–4% Ti alloy is probably due to a strong vacancy–solute interaction energy. On the other extreme, the observation of dislocation loops and helical dislocations in the Cu–2.1% Ti–5% Al alloy would indicate that the vacancies in this alloy are not strongly bound to solute atoms. Thus, by addition of Al, the "easy nucleation" characteristic of the Cu–Ti alloy is altered into the "difficult nucleation" characteristic of the Cu–2.1% Ti–5% Al alloy. Consequently, the latter alloy is associated with a strong tendency for the occurrence of localized precipitation where hetrogenous nucleation occurs at sites of lower activation energy barrier.

Acknowledgement

This paper is based on a thesis submitted towards the partial fulfilment of the requirements for the Ph.D. degree by T. K. Vaidyanathan at the Department of Physical Metallurgy of the Polytechnic Institute of New York.

References

1. U. HÜBNER and G. WASSERMANN, *Z. Metallk.* **53** (1962) 152.
2. H. T. MICHELS, I. B. CADOFF and E. LEVINE, *Met. Trans.* **3** (1972) 667.
3. K. SAITO and R. WATANABE, *J. Phys. Soc. Japan* **22** (1967) 681.
4. S. G. PROKOPINSKAYA and E. V. PANCHENKO, *Izv. Vyssh. Ucheb. Zaved, Tsvet Met.* **10** (1967) 103.
5. J. A. CORNIE, A. DATATTA and W. A. SOFFA, *Met Trans.* 4 (1973) 727.
6. T. MIYAZAKI, E. YAJIMA and H. SUGA, *Trans. JIM* **12** (1971) 121.
7. A. J. ARDELL and R. B. NICHOLSON with an appendix by J. D. ESHELBY, *Acta Met.* **14** (1966) 1295.
8. W. E. KRULL, E. A. STARKE, JUN. and R. W. NEWMAN, *Mat. Sci. Eng.* 9 (1972) 211.
9. A. D. KOROTAYEV, A. T. PROTASON, O. V. TSIMENKO and M. V. LYUBCHENKO, *Fiz. Metal. Mettallov.* **27** (1969) 127.
10. W. GRUHL and H. CORDIER, *Metall* **11** (1957) 928.
11. R. KNIGHTS and W. WILKES, *Acta Met.* **21** (1973) 1503.
12. D. E. LAUGHLIN and J. W. CAHN, *Scripta Met.* 8 (1974) 75.
13. J. H. WESTBROOK, *Z. Krystallogr.* **110** (1958) 21.
14. J. D. EMBURY and R. B. NICHOLSON, *Acta Met.* **13** (1965) 403.
15. M. J. SAARIVIRTA and H. S. CANNON, *Met. Prog.* **76** (1959) 81.
16. G. W. LORIMER and R. B. NICHOLSON, "The Mechanism of Phase Transformations in Crystalline Solids" (Institute of Metals, London, 1969) p. 36.
17. J. E. HILLIARD, "Phase Transformations" (American Society of Metals, Metals Park, Ohio, 1970) p. 497.

Received 14 February and accepted 19 March 1975.